SEMI-ACTIVE CONTROL OF A BRIDGE WITH USE OF A MEGNETORHEOLOGICAL DAMPER

Anat RUANGRASSAMEE[1] and Kazuhiko KAWASHIMA[2]

[1]Member of JSCE, M. Eng., Graduate Student, Dept. of Civil Eng., Tokyo Institute of Technology
(2-12-1 O-okayama, Meguro-ku, Tokyo 152-8552, Japan)
[2]Member of JSCE, Dr. Eng., Professor, Dept. of Civil Eng., Tokyo Institute of Technology
(2-12-1 O-okayama, Meguro-ku, Tokyo 152-8552, Japan)

This study was conducted to investigate the effectiveness of a magnetorheological (MR) damper in the semi-active control of bridge response. Two algorithms to change the damping force according to displacement or velocity were investigated. It is found that the commanded damping force can be realized by the MR damper. However, discrepancy of damping force is observed, when the rate of change of the damping force is high. The shaking table test was conducted on a model bridge with the MR damper to investigate the effectiveness of the control algorithms.

Key Words: *magnetorheological damper, variable damper, semi-active control, preset control algorithm*

1. INTRODUCTION

Semi-active control offers a promising approach for seismic response reduction due to its adjustable damping properties[1]. The recent development of a magnetorheological damper accelerates possible implementation of the semi-active control[2), 3)].

This research was conducted to investigate the effectiveness of a magnetorheological (MR) damper in the semi-active control of bridge response. A series of cyclic loading test was carried out on a MR damper under various loading frequencies, loading amplitudes, and current levels. Two algorithms to vary the damping force according to relative displacement or relative velocity were investigated. The shaking table test was conducted on a bridge model with the MR damper.

2. IDENTIFICATION OF A MR DAMPER

A RD-1005-5-2 MR damper developed by Lord Corporation is used in this study. The damper is 208 mm long in its extended position and 155 mm long in its compressed position. The stroke of the damper is about +/- 25 mm. The cylinder is 41 mm in diameter. The damper operates at the current of 0-2 A. The current is supplied to the damper by a Lord RD-3002 current driver. The current driver outputs a 0-2 A current proportional to a 0-5 V commanded input voltage.

In order to apply the MR damper as a semi-active control device, it is necessary to identify the damping properties of the MR damper. A series of cyclic loading tests was conducted for various loading conditions. Fig. 1 shows the test setup of the cyclic loading test. The damping force was measured by a load cell. The load cell was connected between the reaction frame and the damper. The displacement was measured by a displacement transducer. The current to the damper was controlled by a microcomputer. The commanded voltage was generated by an I/O board which was installed in the computer. Then, the current driver supplied a current proportional to the commanded voltage. A hydraulic actuator with displacement control was used to load the damper.

The damper was loaded under a sinusoidal signal with a fixed frequency and amplitude, while the current to the damper was hold constant. The response of the damper was investigated for a wide range of loading frequencies, loading amplitudes, and current levels. The loading frequencies were 0.5, 1.0, 1.5, 2.0, and 2.5 Hz. The loading amplitudes were 5, 10, 15, and 20 mm. The current levels were 0, 50, 100, 150, 200, 250, 500, and 750 mA.

Fig. 2 shows the response of the MR damper subjected to a 1.5 Hz sinusoidal excitation with the amplitude of 20 mm under the current levels of 0, 250, and 500 mA. It is seen that the damping force increases as the current to the damper increases. The force-displacement relationship of the MR damper is close to that of a friction damper.

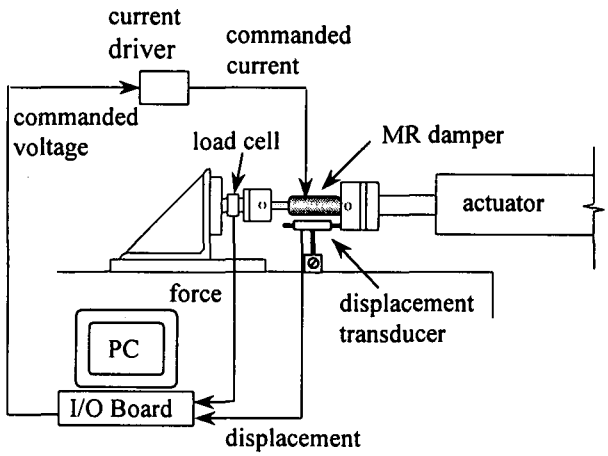

Fig. 1 Test setup of the cyclic loading test

To control the damping force of the MR damper, the model of the MR damper is essential. In this study, the MR damper is modeled by the friction and viscous elements in parallel as shown in Fig. 3. The damping force is expressed as

$$f_d = f + cv \tag{1}$$

where f_d is damping force, f is friction force, c is a damping coefficient, and v is velocity.

From the regression analysis of experimental results, the dependencies of f and c on the current are expressed as

$$f = \begin{cases} 22.6 + 0.267 \times current & ; \quad current < 200mA \\ -53.4 + 0.647 \times current & ; \quad current > 200mA \end{cases} \tag{2}$$

$$c = 0.113 + 0.000327 \times current \tag{3}$$

where f is in N, c is in Ns/mm, and *current* is in mA.

3. CONTROL ALGORITHMS

This study investigates two control algorithms that preset the damping force vs. displacement or velocity relationship. The purpose of the control algorithms is to dissipate energy and to break relative movement between two structures connected by the MR damper.

Fig. 4 shows Algorithm 1 that damping force is commanded as a function of displacement. When the absolute displacement is less than d_1, the damping force is set equal to f_1 that functions to dissipate energy. And when the absolute displacement exceeds d_1, the damping force is commanded to increase linearly to f_2 at d_2. The increase of damping force is intended to break the excessive relative movement.

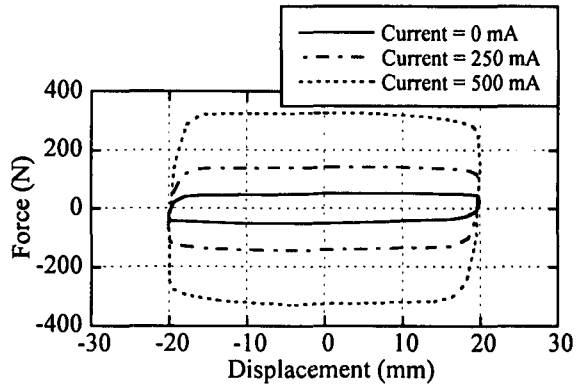

Fig. 2 Force-displacement relationship for a 1.5 Hz sinusoidal excitation

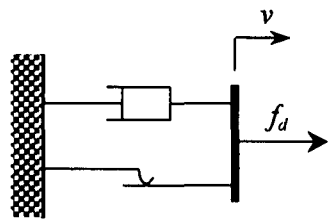

Fig. 3 Idealization of a MR damper

Fig. 5 illustrates Algorithm 2 that the damping coefficient is varied with the displacement and velocity of the damper. When two structures are approaching or moving apart from each other, the displacement and velocity have the same sign. In this case, the damping coefficient is set to a large value c_1. But when the displacement and velocity have the opposite sign, the damping coefficient is set to a small value c_2.

To study the extent to which the control algorithms can be implemented by the MR damper, a series of cyclic loading tests was performed. By applying the model of the MR damper, the control of damping force according to the control algorithm can be made. Algorithm 1 with d_1 = 10 mm, d_2 = 20 mm, f_1 = 80 N, and f_2 = 320 N was tested under the loading frequencies of 0.5, 1.0, 1.5, 2.0, 2.5, and 3.0 Hz and the loading amplitude of 20 mm. And Algorithm 2 with c_1=1.6 Ns/mm, and c_2=0.4 Ns/mm was tested under the same loading conditions.

Fig. 6 and Fig. 7 show the comparison between the measured and commanded force under various loading frequencies for Algorithms 1 and 2, respectively. It is found that the damping force can be produced according to the control algorithms. However, discrepancy of damping force is observed, when the rate of change of the damping force is high. As loading frequency increases, such discrepancy increases. Based on this experimental result, it is worthy to note that the sudden change of damping force as in Algorithm 2 may be difficult to realize in the control and it may cause impact in the damper and the structure.

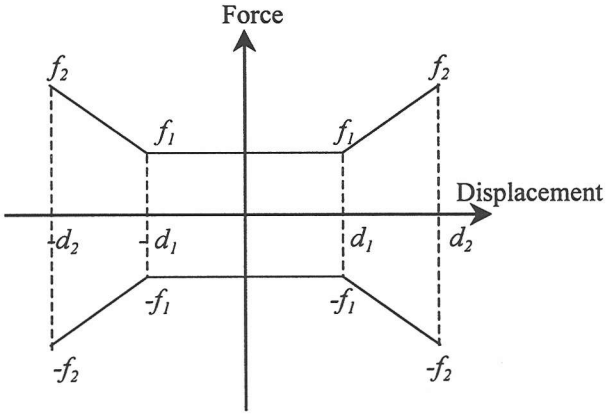

Fig. 4 Algorithm 1

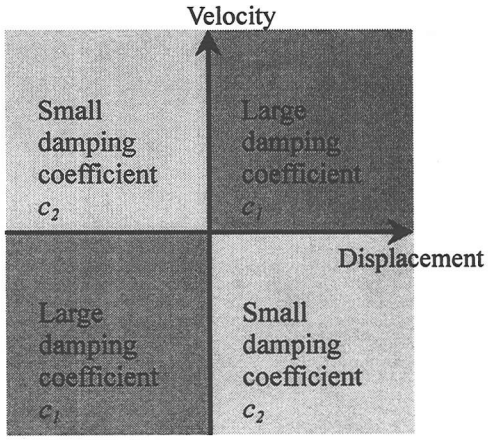

Fig. 5 Algorithm 2

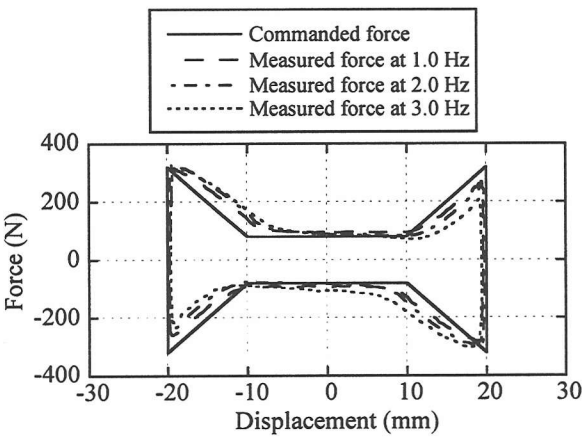

Fig. 6 Measured and commanded force of Algorithm 1

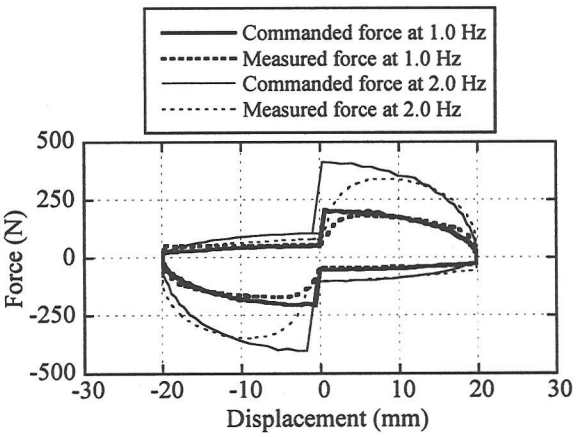

Fig. 7 Measured and commanded force of Algorithm 2

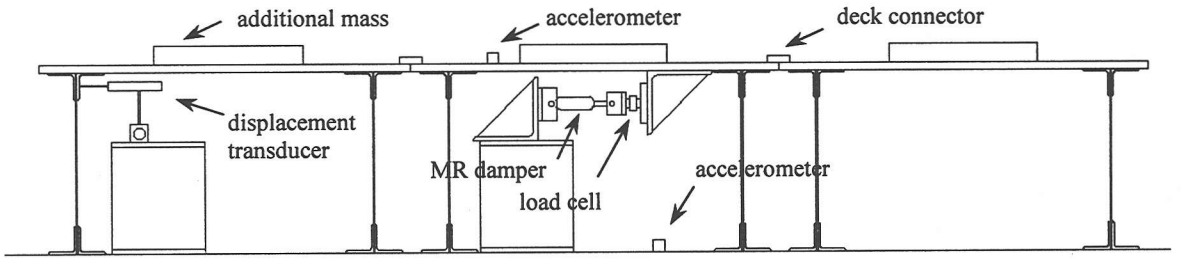

Fig. 8 Bridge model for shaking table test

4. SHAKING TABLE TEST OF A BRIDGE MODEL WITH A MR DAMPER

A shaking table test was performed on a bridge model with the MR damper. The bridge model used in the shaking table test and the measurement is illustrated in Fig. 8. The bridge model was composed of a three-span continuous deck and six piers. The MR damper was connected between the deck and the shaking table. The length of each span was 1.00 m and the height was 0.49 m. The mass of the deck was 370 kg. The deck and piers were made of steel plate and connected together by steel angles. Note that the same piers were used throughout the shaking table test. In some test cases, the piers experienced slight nonlinearity resulting from the stiffness deterioration. A free vibration test of the bridge model without the MR damper was performed. It is found that the natural period is 0.58 s and the damping ratio is 1.2 %. The natural period of the bridge model is a typical value for a standard-size highway bridge.

In the shaking table test, the bridge model was subjected to the NS component of the JMA Kobe record in the 1995 Hyogo-ken Nanbu earthquake. Experimental cases of the shaking table test are listed in Table 1. Intensity of the ground acceleration was scaled down to 5% in the A-series test while it was 8% in the B-series test. The test was conducted in the sequence of A1, A2, A3, A4, A5, B2, B3, B5, B4, and B1.

Table 1 Experimental cases of the shaking table test

Case	Scale of Ground Motion	Control Algorithm	Parameters
A1	5 %	-	current = 0 mA
A2	5 %	1	d_1 = 5 mm, d_2 = 10 mm f_1 = 80 N, f_2 = 160 N
A3	5 %	1	d_1 = 5 mm, d_2 = 10 mm f_1 = 80 N, f_2 = 240 N
A4	5 %	2	c_1 = 1.0 Ns/mm c_2 = 0.4 Ns/mm
A5	5 %	2	c_1 = 1.5 Ns/mm c_2 = 0.4 Ns/mm
B1	8 %	-	current = 0 mA
B2	8 %	1	d_1 = 5 mm, d_2 = 10 mm f_1 = 80 N, f_2 = 160 N
B3	8 %	1	d_1 = 5 mm, d_2 = 10 mm f_1 = 80 N, f_2 = 240 N
B4	8 %	2	c_1 = 1.0 Ns/mm c_2 = 0.4 Ns/mm
B5	8 %	2	c_1 = 1.5 Ns/mm c_2 = 0.4 Ns/mm

Fig. 9 shows the measured damping force for cases B3 and B5. Fig. 10 illustrates the maximum displacement vs. the maximum damping force. It is seen that as the damping force increases the displacement decreases. For both 5% and 8% of the JMA Kobe record, Algorithm 1 can reduce more displacement than Algorithm 2.

5. CONCLUSIONS

The study on the effectiveness of a MR damper for semi-active control of bridge response was conducted. From the investigation presented herein, it may be concluded as

1) The damping force is commanded according to two control algorithms that vary damping force with displacement or velocity. It is found that damping force can be generated according to the control algorithms. However, discrepancy is observed, when the rate of change of the damping force is high and the loading frequency increases.

2) From the shaking table test, it is found that Algorithm 1 provides slightly more reduction of displacement than Algorithm 2 at the same amount of damping force.

ACKNOWLEDGEMENTS: The MR damper used in this study is provided by Sanwa Tekki Corporation. The authors appreciate Dr. Katsuaki Sunakoda and Mr. Hiroshi Sodeyama for their kind cooperation. The authors are thankful to Professor Billie F. Spencer, Jr., University of Notre Dame for his comments. Special thanks are due to Dr. Gaku Shoji, Mr. Gakuho Watanabe, and Mr. Kenji Uehara for their contributions in conducting the cyclic loading test and shaking table test.

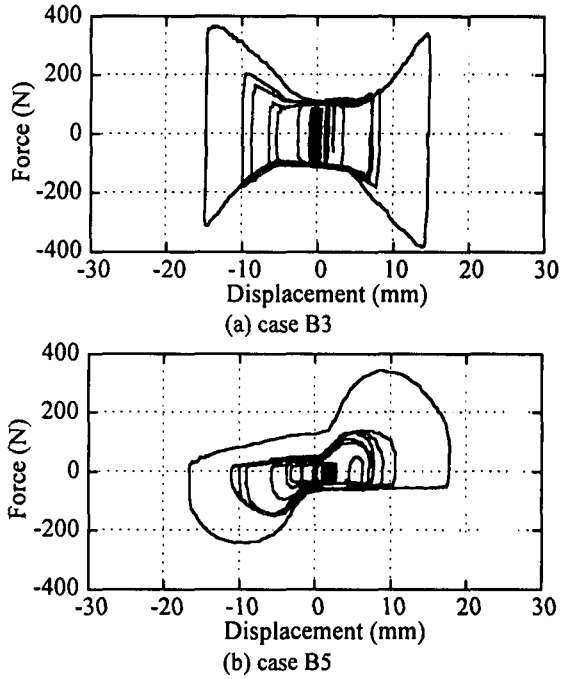

Fig. 9 Damping force under Algorithms 1 and 2

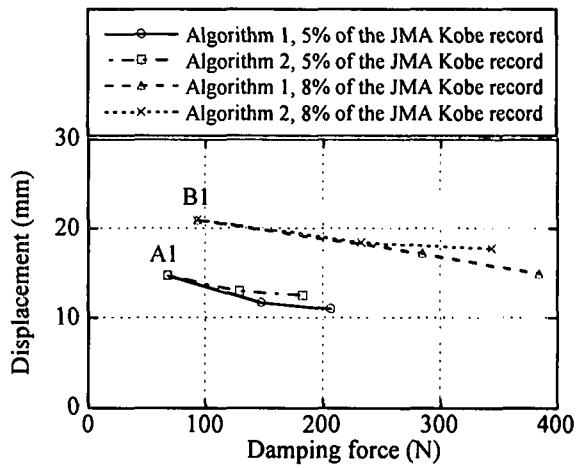

Fig. 10 Comparison of Algorithms 1 and 2

REFERENCES

1) Kawashima, K. and Unjoh, S., Seismic Response Control of Bridges by Variable Dampers, *Journal of Structural Engineering, ASCE*, 120-9, pp. 2583-2601, 1994.

2) Spencer, B. F., Dyke, S. J., Sain, M. K., and Carlson, J. D., Phenomenological Model of a Magnetorheological Damper, *Journal of Engineering Mechanics, ASCE*, 123-3, pp. 230-238, 1997.

3) Sunakoda, K., Sodeyama, H., Iwata, N., Fujitani, H., and Soda, S., Dynamic Characteristics of Magneto-Rheological Fluid Damper, *SPIE 7th Annual Int. Symposium on Smart Structures and Materials*, Newport Beach, USA, 2000.